Front. Optoelectron. China 2010, 3(2): 143–152
DOI 10.1007/s12200-010-0007-y

REVIEW ARTICLE

Prospects and challenges of silicon/germanium on-chip optoelectronics

Erich KASPER (✉)

Institute of Semiconductor Engineering, University of Stuttgart, Stuttgart 70569, Germany

© Higher Education Press and Springer-Verlag Berlin Heidelberg 2010

Abstract On-chip optoelectronics allows the integration of optoelectronic functions with microelectronics. Recent advances in silicon substrate fabrication (silicon-on-insulator (SOI)) and in heterostructure engineering (SiGe/Si) push this field to compact (chipsize) waveguide systems with high-speed response (50-GHz subsystems realized, potential with above 100 GHz). In this paper, the application and requirements, the future solutions, the components and the physical effects are discussed.

A very high refractive index contrast of the waveguide Si-core/SiO_2-cladding is responsible for the submicron line widths and strong bendings realized in chipsize waveguide lines and passive devices. The SiGe/Si heterostructure shifts the accessible wavelength into infrared up to telecommunication wavelengths 1.30–1.55 µm. Germanium, although also an indirect semiconductor as silicon, offers direct optical transitions which are only 140 meV above the dominant indirect one. This is the basic property for realizing high-speed devices for future above 10 GHz on-chip clocks and, eventually, a laser source monolithically integrated on the Si substrate.

Keywords optoelectronics, semiconductor circuit, silicon germanium, silicon-on-insulator (SOI), photodetector, modulator, waveguide, quantum confined Stark effect (QCSE)

1 Introduction

Silicon (Si) is the material choice for microelectronics because it offers many good or acceptable electrical properties (often not the best ones), but its integration degree surpassed that of other material systems by several orders of magnitude. The optoelectronic properties of silicon are, especially with respect to emission and absorption, not that favorable than those of III/IV semiconductors because silicon is an indirect semiconductor. Indirect semiconductors have rather low optical transition probabilities because the momentum conservation needs the involvement of a large momentum, low-energy phonon.

For integration of microelectronics with optoelectronics, however, the use of on-Si-based solution is mandatory. The integration of photo-detectors with electronic circuitry was already very successfully implemented for large-pixel-number vision systems (cameras). Within a decade, the conventional way of image detection and storage was wiped out and replaced by opto-/microelectronics on Si, generating a new large industry branch.

Will this integration of micro- and optoelectronic functions continue to be a motor of innovation? The answer is yes because there are urgent consumer needs and novel technical possibilities to satisfy them.

Modern information societies need high-speed access to the home (fiber to the home connected with high-speed optical to electrical conversion) and high-speed mobile computing. High-speed computing requires on-chip optical interconnects for above 10-GHz clock frequency and ultrafast date exchange between multi-cores and between logic and memory cells.

The technical response to these requirements is driven by two material/device advancements:

i) Extreme high index contrast wave guiding is allowed by a silicon-based substrate technology (silicon-on-insulator (SOI));

ii) Emission, detection, wavelength and speed properties of Si may be improved by several orders of magnitude by lattice-mismatched heterostructures of germanium (Ge)-on-Si.

2 Applications and requirements

Basically, three different scenarios hold for the application spectrum, and they determine the most important requirements.

Received November 24, 2009; accepted December 23, 2009

E-mail: kasper@iht.uni-stuttgart.de

i) Scenario A: passive detection of light by a high pixel number (imaging).

The detection of visible light by charge-coupled devices (CCDs) or complementary metal oxide semiconductor (CMOS) transistor circuit is now ubiquitous in mobile phone cameras, surveillance and consumer/industrial photographer equipment. Each pixel in a CMOS image sensor consists of a photodiode (part of the CMOS process) and a read-out transistor (passive pixel sensor), or with additional reset/amplifier transistors (active pixel sensor) or with an analog/digital converter (ADC), a digital signal processor (DSP) and a memory (digital pixel sensor).

For the read-out and intelligent processing, the silicon circuit is ideal, but for the photo diode, a better absorbing material would be preferred to decrease the pixel size, increase speed and extend the spectral range. In Fig. 1, a Ge-on-Si detector array (together with CMOS logic and mm-wave radar) is shown which would allow night vision (wavelength in the infrared up to 1.55 μm) and very small pixel size with high resolution. This is intended for an automotive warning system for small and less visible objects.

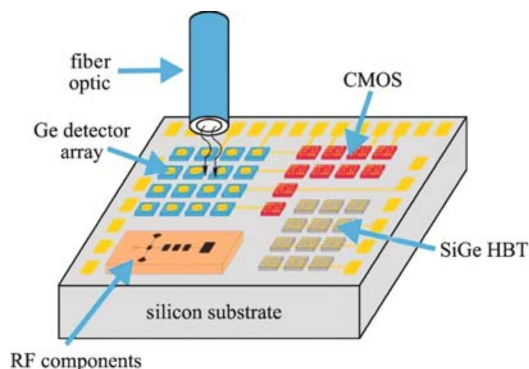

Fig. 1 Integrated Ge detector array for night vision (HBT: heterojunction bipolar transistor; RF: radio frequency)

ii) Scenario B: separate transmitter and receiver chips.

This is valid for chip-to-chip or board-to-board connections. Mainly vertical light emitters for the transmitter chip are required. A high freedom for wave length choice (visible to infrared) and fiber type (glass, plastic) is allowed.

iii) Scenario C: on-chip interconnects and signal transmission.

Here all elements (sources, waveguides, modulations, detectors, filters, etc.) have to be integrated in an appropriate form. A high degree of monolithic integration is favored. The application spectrum of these solutions ranges from replacement of electrical on-chip clock for beyond 10-GHz computing, to fast data exchange in system-on-chip (SOC) between logic cores and embedded memories or between cores in multi-core logic, to contactless separation of different voltage supply blocks (periphery, CMOS logic, smart power) and to all optical switching/computing.

3 Near-future solutions

For application-driven solution, several boundary conditions have to be considered. The most important one concerns the choice of the wavelength.

The wavelength can either be dictated by the applications (1.30–1.55 μm for telecommunication, visible plus near infrared for detector arrays) or be chosen taking into account the most convenient technical solutions. The choice may be determined by the easily available light sources or by the transparency regime of the chosen waveguide system. For instance, as light source, a GaAs laser at 850 nm for board-to-board communication or a broadband visible silicon light source [1] for silicon oxide/silicon nitride waveguide system on top of the metallization can be chosen. The visible silicon light source is based on the recombination of hot carriers in a highly reverse biased p/n junction. Avalanche multiplication provides carriers of both types to generate visible light detectable with the naked eye [1]. The detector and some types of modulation have to be made from materials which absorb in the transparency region of the waveguide material system.

For near-future solutions, the author recommends two approaches (Table 1).

The second system could be the most sustainable if future integrated circuit (IC) generations move toward replacement of the bulk silicon substrate by SOI substrates.

A general scheme of an on-chip interconnect system based on this proposal is given in Fig. 2. The waveguide is silicon surrounded by oxide. This is a high refractive index contrast system which allows sharp bending and sub-micron width dimensions. The laser light (1.10–1.55 μm) is coupled in via a waveguide grading coupler on a tapered planar waveguide. The detector/modulators are made from Ge-on-Si, which absorbs in the chosen wavelength region.

Table 1 Near-future solutions of silicon-based source/waveguide/detector system

approaches	waveguide material	waveguide position	light source	detector/modulator material
1	siliconoxide/-nitride	top of metallization	reverse p/n, visible	silicon p/n
2	SOI	bottom of metallization	fiber, infrared, coupled in	Ge-on-Si

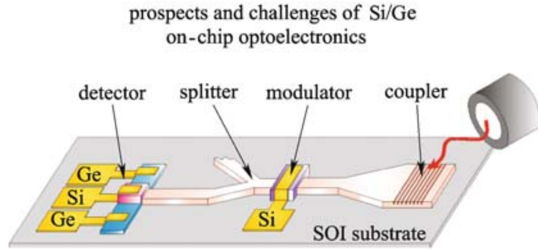

Fig. 2 On-chip interconnect on SOI substrate (laser light (infrared, above 1.1 μm) is coupled into a tapered grading waveguide)

4 Components and physical effects

The backbone of an on-chip optical communication/interconnect system is the optical waveguide which, in simplest form, is a straight line connecting two points but includes also different forms of passive waveguide devices as couplers, combiners, dividers, resonators, delay lines, gratings, and filters. This waveguide system distributes the optical signal around the chip in dependence of its wavelength and polarization.

Mainly at the ends of such a passive waveguide system (Fig. 3) active devices are needed as light sources, intensity modulators and detectors.

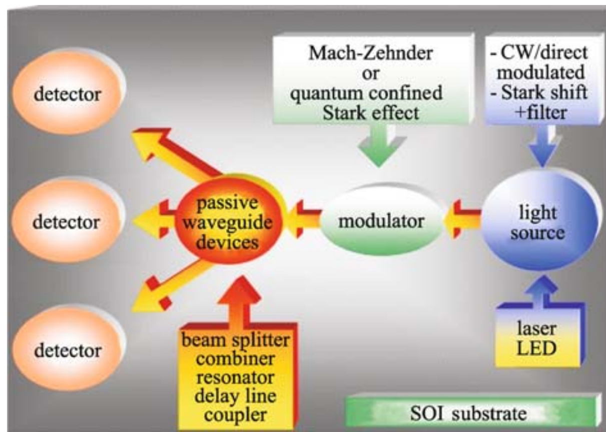

Fig. 3 On-chip concept of a waveguide system on SOI (CW: continuous wave; LED: light emitting diode)

4.1 SOI waveguides

For optical dielectric waveguides, a core/cladding structure is required with a core of higher index of refraction, as, for instance, best known from the optical fiber. An important design criterion for waveguide is the (refractive) index contrast which should be high to shrink the dimensions. Index contrast ranges from percent in the classical fiber to up to 10% between different semiconductors (III/V material, SiGe/Si [2]) and highest (more than 50%) in semiconductor/insulator couples. In SOI, the index contrast between Si ($n \approx 3.5$) to SiO_2 ($n \approx 1.5$) is that high (Fig. 4) ($\Delta n/n \approx 65\%$) that submicron waveguides are possible [3,4].

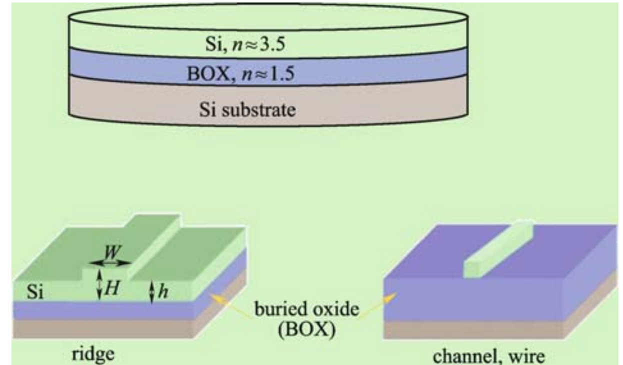

Fig. 4 Optical waveguides on SOI

4.2 Passive waveguide devices

For an overview about the diversity of passive waveguide devices, see recent papers [5]. As an example, we discuss here the grating coupler which allows coupling of light from a fiber into the on-chip waveguide system (Fig. 5). This coupler is composed of four parts: the monomode fiber is inclined about 10° to the vertical, and light shines on the linear grating which is placed on the end of a planar waveguide taper which confines the waves to a nanowire[1)] [6].

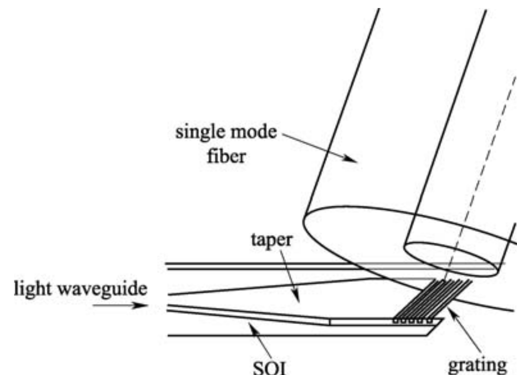

Fig. 5 Grating coupling from a fiber into a tapered planar waveguide [3]

The conditions for Bragg reflections are given by

$$k_x = \frac{2\pi}{\lambda_0} n_{\mathrm{eff}} + m\frac{2\pi}{p}, \tag{1}$$

where k_x, λ_0, n_{eff}, p, and m are the incoming wave vector

1) Yu J, Huang Q, Xu X, Xiao X, Zhu Y, Liu Y, Li Z, Li Y, Fan Z, Yu Y. SOI based waveguide devices. Submitted

component in waveguide direction, wavelength, effective index of refraction, grating period length, and order of reflection ($m=-1,-2,\ldots$), respectively.

$$k_x = \frac{2\pi}{\lambda_0}\sin\theta, \qquad (2)$$

with the inclination angle θ.

For a given wavelength λ_0 and grating period length p, the requirements on the effective index of refraction and the inclination angle may be assessed by

$$n_{\text{eff}} - \sin\theta = -\frac{m\lambda_0}{p}. \qquad (3)$$

By adding the index buffer layer, the diffractive grating becomes more directional, and the reflections between the fiber facet and the grating surface are reduced. Coupling efficiencies around 50% can be obtained.

4.3 Modulator

Signal modulation can be achieved very simply by switching on/off the light sources. In reality, this direct modulation limits the performance of the light emitter especially in integrated devices. Therefore, often, the signal modulation is splitted between two devices: a light emitter running as continuous wave (CW) source and a following modulator where performance can be optimized.

Two basic modulation principles are applied.

i) Interference modulation by electrically stimulated phase changes in the two branches of an interferometer. The well-known prototype following this principle is given by the Mach-Zehnder interferometer (MZI). In one or both branches of the MZI (Fig. 6), a phase shifter is installed.

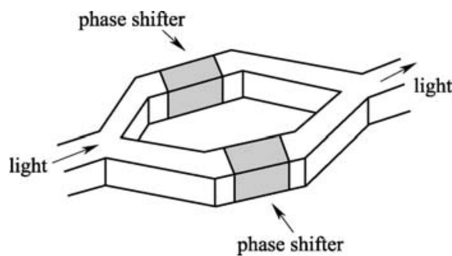

Fig. 6 Mach-Zehnder interferometer with electrically stimulated phase shifter

A phase shifter allows switching the output between constructive and destructive interferences. The commonly used phase shifter varies the optical length,

$$l_{\text{opt}} = ln, \qquad (4)$$

by changing the refractive index n. This can be accomplished by injection of carriers into the depletion region of a junction.

The physical process is described as free carrier absorption (Fig. 7). The injected carriers increase the absorption without any energy cutoff because carriers in the conduction (valence) band are lifted to higher energies in the same band (Fig. 8).

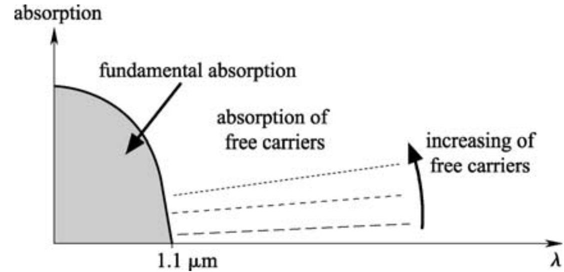

Fig. 7 Absorption in semiconductors (fundamental absorption (band-band absorption) and free carrier absorption)

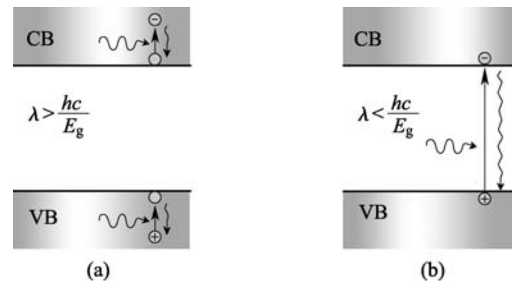

Fig. 8 Absorption mechanism. (a) Free carrier absorption; (b) fundamental absorption (band-band) (CB: conduction band; VB: valence band)

The absorption at 1.55-μm wavelength is given by

$$\Delta\alpha = 8.5\times10^{-18}\Delta N_{\text{e}} + 6.0\times10^{-18}\Delta N_{\text{h}}, \qquad (5)$$

where absorption coefficient α is in cm^{-1}, and electron (hole) density $N_{\text{e}}(N_{\text{h}})$ is in cm^{-3}.

The Kramers-Kronig rule [7] links small changes in the absorption to changes in the index of refractionΔn,

$$\Delta n = -[8.8\times10^{-22}\Delta N_{\text{e}} + 8.5\times10^{-18}(N_{\text{h}})^{0.8}], \qquad (6)$$

where the index change Δn is small requiring large lengths of the phase shifter which make the MZI not very integration friendly. The optical structure of integrated interferometer structures uses preferably multiple reflections (Fabry-Perot cavity) or multiple path usage (mirroring or micro disc with high quality (Q)-factor).

ii) The second principle uses the absorption modulation near the band edge by an applied electric field. These effects are known as Franz-Keldysh effect in bulk semiconductors or quantum confined Stark effect (QCSE) in quantum well structures. (Remark to history: The German physicist Stark discovered around 1930 the energy shift of molecule lines in an electric field, the Russian researchers Franz and Keldysh found and

described the influence of electric fields on the absorption band edge around 1950, and with modern quantum structures, the similarity between atoms/molecules and low-dimensional structures was rediscovered.)

The red shift of absorption in a quantum well (QCSE) can easily be explained looking at Fig. 9. Without electric field ($F=0$), the absorption edge is given by the band gap of the well material plus the quantization energy of the confined carriers. With electric field F, the effective energy gap becomes smaller (see Fig. 9(b)) outweighing the higher confinement energy of the triangular well. The absorption modulators operate with wavelengths slightly higher than the absorption edge of the chosen modulator material. Without field, the signal runs through, and with electric field, the absorption increases which allows modulator lengths below 10 μm.

The advantage of absorption modulators concerns small sizes, low power consumption (reverse field with low carrier injection) and high-speed potential. The main problem is the exact band gap adjustment.

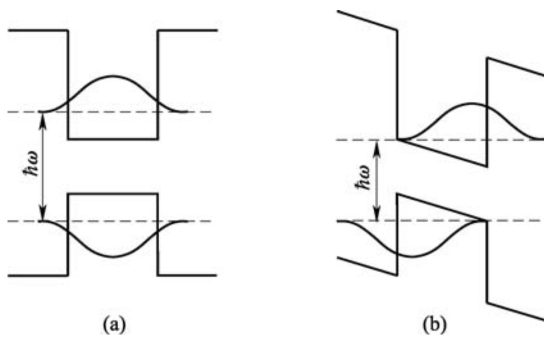

Fig. 9 Quantum confined Stark effect (QCSE)

4.4 Light emitters

Silicon light emitters suffer from low quantum efficiency in indirect semiconductors which stimulated tremendously the search for unique solutions. Main directions are either dominated by technological efforts to use the effective III/V laser sources (hybrid laser mounting on Si or external laser with fiber/waveguide coupling) or basic physical approaches which should overcome the indirect semiconductor limitations. The later approach could be used to integrate monolithically light emitters on silicon. These approaches are mainly based on three principles.

i) Limitations of the wavevector (k-space) by nanostructures.

ii) Utilization of localized states (defects) to overcome the need for phonon help in indirect transitions.

iii) Modification of Ge (on Si) to shift this only weekly indirect semiconductor to a direct one.

Nanostructures (ad i): The basic idea is explained on the Si/Ge superlattices. A periodic ultrathin superlattice reduces the first Brillouin zone in the growth direction. The reduced wavevector length $k_{\text{SLS}} = \pm\pi/L$ (Brillouin zone folding) gives rise to minibands which show at an appropriate chosen superlattice period length L a pseudo-direct transition [8]. The appropriate superlattice period length L is given by multiples of $2.5a$ (a is Si lattice constant, $a = 0.543$ nm) because the energy minimum of (100) Si electrons is at about $(2\pi/a)(1-0.2)$. These ultrathin superlattices are very demanding on growth technique; Zachai [9] could prove the existence of pseudodirect transitions in 10 ML (monolayer, ML, 1 ML $= a/4$) Ge/Si superlattices, but the transition strength was not high enough for laser action. Progress since then (with quantum dots, nanocrystals, porous Si) is continuing [10,11] but suffering from rather low intensities.

Defects (ad ii): With localized defects, the radiative transition does not need the help of phonons. Several approaches (ion implantation, Er incorporation) were tried, and the most promising could be the fabrication of a dense regular network of dislocation (Fig. 10) by direct wafer bonding [12].

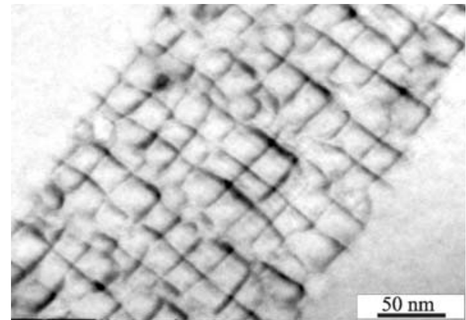

Fig. 10 Light sources in Si (detail: dislocations) [12]

Modified Ge (ad iii): The group IV semiconductor diamond, SiC, Si, and Ge are all indirect semiconductors with decreasing bandgap as the lattice constant expands. The lowest direct transition is about 2.3 eV above the indirect (X-direction) one in Si. However, in Ge, the direct one is only 140 meV above the indirect (L-direction). Ge is very near to get a direct semiconductor (Fig. 11). The route via Ge seems the most promising to get an efficient Si-based light source or laser.

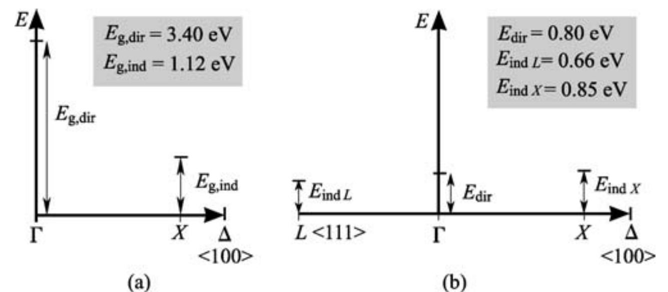

Fig. 11 Scheme of important indirect and direct band transitions. (a) In Si; (b) in Ge

The modifications of Ge now discussed very seriously contain tensile strain, high doping, and GeSn alloys.

5 High-speed photodetectors

Photodetectors convert the optical signal into an electrical one. Several properties of the detector have to be considered (Table 2). Here we especially focus on the time response, and the resulting frequency bandwidth is investigated in more detail because within a few years, a dramatic increase of the speed of Si/Ge photodetectors to up to 50 GHz was obtained. These allow the realization of high-speed optoelectronic circuits on Si.

Table 2 Important photodetector parameters

	parameter
1	quantum efficiency
2	noise
3	time response/frequency bandwidth
4	dynamic range
5	spectral response
6	linearity
7	size and numbers of pixels
8	operation temperature

The photon detection principle mainly used with semiconductors is based on band-to-band absorption and separation of the generated electron-hole pair in the electric field of a junction (photodiode). All junctions with a depletion layer can be used, such as p/n-junction, Schottky-diode junction, metal insulator semiconductor (MIS) junction, and metal insulator metal (MIM) junction. The basics are explained on the example of a pin diode. The uniform electric field F in the intrinsic region is given approximately by

$$F = (V_{\mathrm{bi}} - V)/w_{\mathrm{D}}, \tag{7}$$

where V, V_{bi} and w_{D} are the applied voltage, the built-in voltage, and the thickness of the intrinsic drift region, respectively.

After absorption of a photon of energy $h\nu > Eg$, an electron-hole pair is created (fundamental absorption in semiconductors). The electron-hole pairs are immediately separated by the electric field F if the absorption takes place in the intrinsic region leading to a photocurrent I_{ph}. Absorption outside the intrinsic region leads only to a photocurrent if the minority carriers manage to diffuse to the intrinsic region (Fig. 12).

Technically, the photodetectors can be arranged for vertical incidence (imaging with detector arrays, chip-to-chip or board-to-board communication) or for lateral incidence (fiber-to-chip, on-chip communication). The

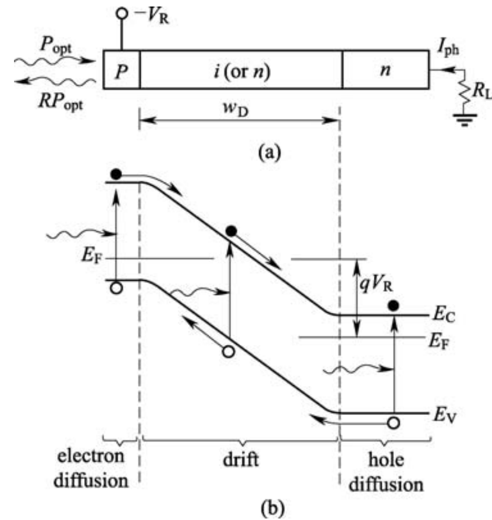

Fig. 12 Operation of photodiode. (a) Cross-section view of p-i-n diode; (b) energy-band diagram under reverse bias [13]

breakthrough work on lateral incidence SiGe/Si photodetectors was done already in 1994 [14]. A Daimler/University cooperation led by Kasper E and Petermann K combined a ridge waveguide (SiGe on bulk Si) with a lateral pin detector, the depletion region of which was composed of a SiGe/Si superlattice (Fig. 13).

Let us now concentrate on the reason for the astonishing rapid increase on speed of Ge/Si photodetectors in the low mm-wave regime (30–45 GHz). Our group [15] leads the race with measured 49 GHz (Remark: The measurement by S-parameter network analyzer includes the speed of the detector and the delay caused by the laser light modulator, so the real speed of the detector is somewhat higher, about 60–70 GHz). The most important measure is to suppress the slow minority carrier diffusion from absorption outside the depletion layer (Fig. 14).

This is accomplished by a combination of three technological steps [16]:

i) Very abrupt junction. Transition of the highly doped contact layers to the intrinsic layer (several orders of magnitude difference in doping) is within a few nanometers.

ii) High doping ($>10^{20}\,\mathrm{cm}^{-3}$) of the contact layers to reduce carrier lifetime.

iii) A misfit dislocation network at the bottom contact which also reduces lifetime of minority carriers.

The diffusion length L of minority carriers is given by

$$L^2 = D\tau = q\mu\tau, \tag{8}$$

where q, D, μ, and τ are the electric charge of the electron, the diffusion coefficient, the mobility, and the minority carrier lifetime, respectively.

At high doping, the diffusion length is reduced by the low mobility (factor 30 lower than in undoped material).

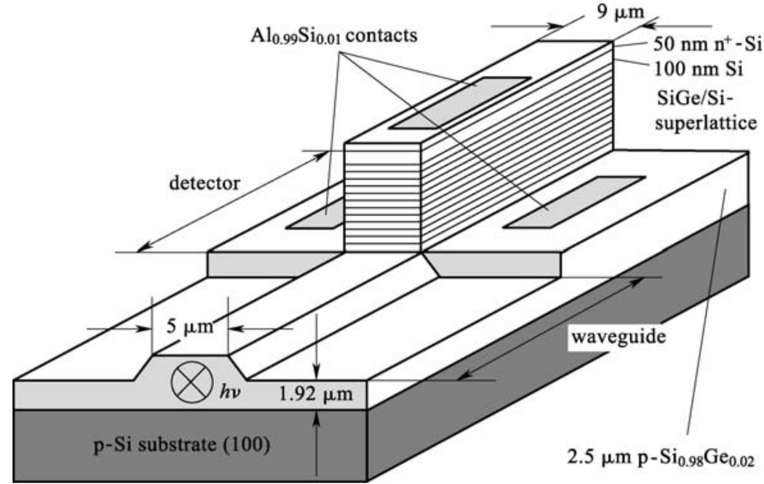

Fig. 13 Lateral-incidence detectors

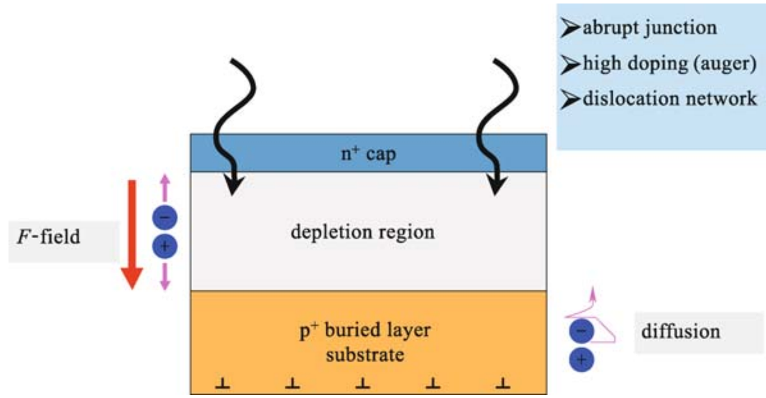

Fig. 14 Suppression of (slow) carrier diffusion

The low minority carrier lifetime is caused by the auger effect where the momentum of the recombining electron (hole) is transferred to a nearly available electron (hole).

The detector speed is dominated by two effects if the slow diffusion is suppressed.

i) Internal speed of the device is given by the transit time. Assuming a saturation velocity v_s of carriers in the depletion region, the internal frequency band f_{tr} is given by the simple expression [17]

$$f_{tr} = \frac{\sqrt{2}}{\pi}\frac{v_s}{w_D}, \quad (9)$$

where v_s and w_D are the saturation velocity ($v_s = 0.6 \times 10^5$ m/s in Ge) and drift width (the intrinsic width in abrupt junctions), respectively.

The assumption of saturation velocity is correct if the field strength F is more than about 3×10^6 V/m (e.g., with $V_{bi} - V = 1$ V, $w_D = 300$ nm, the field strength $F = 3 \times 10^6$ V/m).

ii) The connection to the outer world (measurement surrounding) is limited by the RC load given by the capacitance C_j of the device and by the resistance of the connection line $(R_S + 50)\Omega$ (R_S is the series resistance; 50 Ω is the waveguide measurement impedance):

$$f_{RC} = \frac{1}{2\pi R C_j} = \frac{1}{2\pi}\cdot\frac{w_D}{A\varepsilon(R_S + 50)}. \quad (10)$$

The 3-dB bandwidth f_{3dB} is roughly given by a superposition [17]:

$$\frac{1}{{f_{3\,dB}}^2} = \frac{1}{{f_{tr}}^2} + \frac{1}{{f_{RC}}^2}. \quad (11)$$

The influence of RC load is shown in Fig. 15, where a 50-GHz internal speed detector is loaded with different capacitances C_j.

From these investigations, we concluded the dependence of vertical detector speed [17,18] on the thickness of intrinsic zone and device mesa radius (Fig. 16).

The results demonstrate that with small pixel devices (4-µm diameter), speeds far above 100 GHz should be

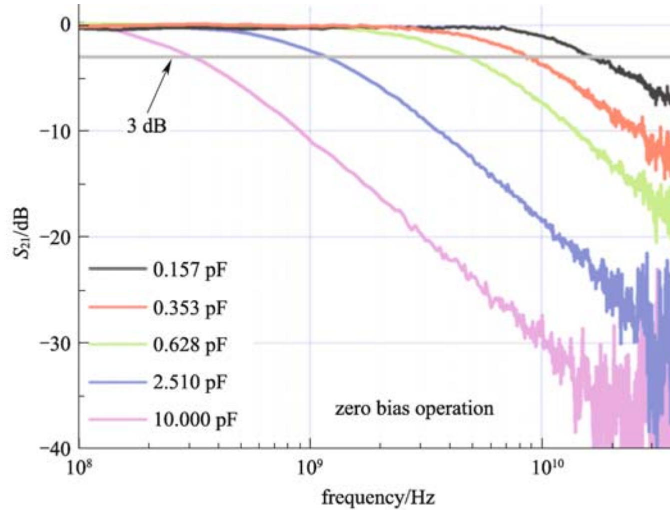

Fig. 15 Response versus frequency for differently loaded detectors of the same internal structure (50-GHz detector)

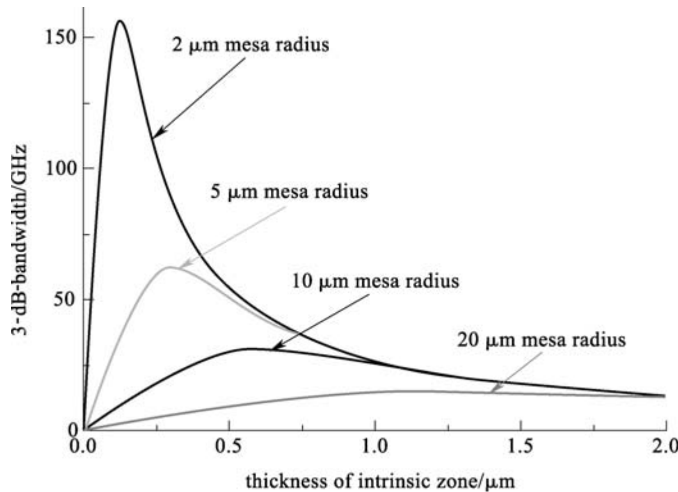

Fig. 16 Theoretical 3-dB bandwidth of vertical Ge/Si photodetectors

obtained ready for 160-Gbit/s communication on-chip.

The speed of properly designed Ge-on-Si detectors is obtained already at low reverse bias (Table 3). Ge is a small band-gap semiconductor which is always connected with much higher dark currents than usual in Si. In order to minimize dark currents, an operation of the device at zero bias is highly appreciated. Our group obtained very good results with zero-bias operation due to the very abrupt junctions grown by molecular beam epitaxy (MBE).

6 Heterostructure engineering

Combining different thin semiconductor layers on a common substrate is called heterostructure engineering. The different electronic and optical properties of heterostructures allow to extend the wavelength regime or to combine transparent waveguides with absorbing emitter, modulator, and detector structure.

The realization of heterostructures in group IV materials (as Si) is especially complicated because the change in electronic properties is related completely to a change in bond length. Combination of materials with different bond lengths gives lattice-mismatched interfaces. The engineering of lattice-mismatched heterostructures is a hot topic in material science and device physics. For a rigorous treatment of the related phenomenon with SiGe/Si lattice-mismatched structures, the reader is referred to books on this matter [26–29].

The most important consequences are as follows:

i) Very thin layers of lattice-mismatched structures [30] are completely strained to match the substrate lattice planes (typical thickness is in the 10-nm range).

ii) Strain adjustment can be obtained by the so-called

Table 3 3-dB frequencies $f_{3\,\mathrm{dB}}$ of photo-detectors (compared are detectors with reverse bias and zero-bias detectors)

organization	bias/V	$f_{3\,\mathrm{dB}}$/GHz	wavelength/nm	year
IBM [19]	−4	29	850	2004
MIT [20]	−3	12.1	1540	2005
LETI [21]	−2	35	1310/1550	2005
USTUTT [22]	−2	39	1550	2005
LUXTERA [23]	−1	>20	1554	2007
LETI [24]	−4	42	1550	2008
ETRI [25]	−3	35	1550	2008
USTUTT [15]	−2	49	1550	2008
USTUTT[22]	zero	25	1550	2005
USTUTT [15]	zero	39	1550	2008

virtual substrates which consist of silicon substrate with a thin, but strain relaxed buffer layer of different composition (mainly SiGe).

iii) Strain is a very powerful method to modify the electronic and optical properties of a thin layer.

7 Outlook

The progress in special substrate technology (SOI) and in heterostructure engineering (SiGe/Si) provides excellent new tools to push the monolithic integration of optoelectronic and microelectronic functions on Si in a very systematic manner.

Near-term benefits will be in the areas of fiber to the home, fast computers, infrared imaging, and smart power.

On a larger timescale, all optical signal processing, direct image conversion and medical- and biosensor arrays will be in the focus.

Acknowledgements This overview is based on work done at the Institute of Semiconductor Engineering at University Stuttgart, Germany. The author would like to acknowledge the help of the MBE group and the device technology group. Many thanks are due to Oehme M, Kaschel M and Xu H for stimulating discussions and help with data collection. The sections on passive waveguide devices and system aspects benefitted from cooperation and exchange with the groups and students of my Chinese colleagues Yu Jinzhong and Zhang Xinliang.

References

1. Morschbach M, Oehme M, Kasper E. Visible light emission by a reverse-biased integrated silicon diode. IEEE Transactions on Electron Devices, 2007, 54(5): 1091–1094
2. Splett A, Schüppert B, Petermann K, Kasper E, Kibbel H, Herzog H J. Waveguide pin photodetector combination in SiGe. In: Proceedings of OFC/IOOC Technical Digest Series. 1993, 4: 116–117
3. Taillaert D, Bogaerts W, Bienstman P, Krauss T F, Van Daele P, Moerman I, Verstuyft S, De Mesel K, Baets R. An out-of-plane grating coupler for efficient butt-coupling between compact planar waveguides and single-mode fibers. IEEE Journal of Quantum Electronics, 2002, 38(7): 949–955
4. Bogaerts W, Dumon P, Brouckaert J, De Vos K, Taillaert D, Van Thourhout D, Baets R. Ultra-compact optical filters in silicon-on-insulator and their applications. In: Proceedings of the 4th IEEE International Conference on Group IV Photonics. 2007, 1–3
5. Yu J, Yu H J, Zhu Y, Yu Y D. Theoretical and experimental studies of an ultra-compact photonic crystal corner mirror based on silicon-on-insulator. In: Proceedings of the 5th IEEE International Conference on Group IV Photonics. 2008, 222–224
6. Zhu Y, Li Z Y, Han W H, Fan Z C, Yu Y D, Yu J Z. High efficiency silicon-on-insulator grating coupler between submicron waveguides and fibers. Proceedings of SPIE, 2009, 7516: 75160A
7. Klingshirn C F. Semiconductor Optics. Berlin: Springer-Verlag, 2005
8. Gnutzmann U, Clausecker K. Theory of direct optical transitions in an optical indirect semiconductor with a superlattice structure. Applied Physics A, 1974, 3(1): 9–14
9. Zachai R, Eberl K, Abstreiter G, Kasper E, Kibbel H. Photoluminescence in short period Si/Ge strained layer superlattices grown on Si and Ge substrates. Surface Science, 1990, 228(1–3): 267–269
10. Pavesi L, Dal Negro L, Mazzoleni C, Franzo G, Priolo F. Optical gain in silicon nanocrystals. Nature, 2000, 408(6811): 440–444
11. Cloutier S G, Kossyrev P A, Xu J. Optical gain and stimulated emission in periodic nanopatterned crystalline silicon. Nature Materials, 2005, 4(12): 887–891
12. Kittler M, Reiche M, Arguirov T, Seifert W, Yu X. Silicon-based light emitters. Physica status solidi A, 2006, 203(4): 802–809
13. Sze S M, Ng K K. Physics of Semiconductor Devices. 3rd ed. New York: Wiley, 2006
14. Splett A, Zinke T, Petermann K, Kasper E, Kibbel H, Herzog H J, Presting H. Integration of waveguides and photodetectors using SiGe multi-quantum-wells with triangular shaped Ge-profile. In: Proceedings of Integrated Photonics Research, 1994, 3: 149–150
15. Klinger S, Berroth M, Kaschel M, Oehme M, Kasper E. Ge on Si p-i-n photodiodes with a 3-dB bandwidth of 49 GHz. IEEE Photonics Technology Letters, 2009, 21(13): 920–922
16. Kaschel M, Oehme M, Kirfel O, Kasper E. Spectral responsivity of

fast Ge photodetectors on SOI. Solid-State Electronics, 2009, 53(8): 909–911
17. Oehme M, Werner J, Kasper E, Jutzi M, Berroth M. High bandwidth Ge p-i-n photodetector integrated on Si. Applied Physics Letters, 2006, 89(7): 071117
18. Oehme M, Werner J, Kasper E, Klinger S, Berroth M. Photocurrent analysis of a fast Ge p-i-n detector on Si. Applied Physics Letters, 2007, 91(5): 051108
19. Dehlinger G, Koester S J, Schaub J D, Chu J O, Ouyang Q C, Grill A. High-speed germanium-on-SOI lateral PIN photodiodes. IEEE Photonics Technology Letters, 2004, 16(11): 2547–2549
20. Dosunmu O I, Cannon D D, Emsley M K, Kimerling L C, Ünlü M S. High-speed resonant cavity enhance Ge photodetectors on reflecting Si substrates for 1550-nm operation. IEEE Photonics Technology Letters, 2005, 17(1): 175–177
21. Rouvière M, Vivien L, Le Roux X, Mangeney J, Crozat P, Hoarau C, Cassan E, Pascal D, Laval S, Fédéli J M, Damlencourt J F, Hartmann J M, Kolev S. Ultrahigh speed germanium-on-silicon-on-insulator photodetectors for 1.31 and 1.55 μm operation. Applied Physics Letters, 2005, 87(23): 231109
22. Jutzi M, Berroth M, Wöhl G, Oehme M, Kasper E. Ge-on-Si vertical incidence photodiodes with 39-GHz bandwidth. IEEE Photonics Technology Letters, 2005, 17(7): 1510–1512
23. Masini G, Capellin G, Witzens J, Gunn C. A 1550 nm, 10 Gbps monolithic optical receiver in 130 nm CMOS with integrated Ge waveguide photodetector. In: Proceedings of the 5th IEEE International Conference on Group IV Photonics. 2007, 28–30
24. Vivien L, Marris-Morini D, Mangeney J, Crozat P, Cassan E, Laval S, Fédéli J M, Damlencourt J F, Lecunff Y. 42 GHz waveguide germanium-on-silicon vertical PIN photodetector. In: Proceedings of the 5th IEEE International Conference on Group IV Photonics. 2008, 185–187
25. Suh D, Kim S, Joo J, Kim G, Kim I G. 35 GHz Ge p-i-n photodetectors implemented using RPCVD. In: Proceedings of the 5th IEEE International Conference on Group IV Photonics. 2008, 191–193
26. Kasper E. Properties of Strained and Relaxed Silicon Germanium. London, UK: Institution of Electrical Engineers, 1995
27. Kasper E, Paul D J. Silicon Quantum Integrated Circuits—Silicon-Germanium Heterostructure Devices: Basics and Realisations. Heidelberg: Springer-Verlag, 2005
28. Kasper E, Klingshirn C. Semiconductor Quantum Structures: Optical Properties of Group IV Semiconductors. Optical Properties 3, Landolt Börnstein, New Series. Berlin: Springer-Verlag, 2007
29. Kasper E, Müssig H J, Grimmeiss H G. Advances in Electronic Materials. Materials Science Forum. Zürich: TransTech Publications, 2009
30. Yu J, Kasper E, Oehme M. 1.55-μm resonant cavity enhanced photodiode based on MBE grown Ge quantum dots. Thin Solid Films, 2006, 508(1–2): 396–398